

# Side reactions and stability of pre-treated carbon felt electrodes for vanadium redox flow batteries: A DEMS study

L. Eifert<sup>a</sup>, Z. Jusys<sup>b</sup>, R.J. Behm<sup>b</sup>, R. Zeis<sup>a, c, \*</sup>

<sup>a</sup> Karlsruhe Institute of Technology, Helmholtz Institute Ulm, Helmholtzstraße 11, D-89081, Ulm, Germany

<sup>b</sup> Institute of Surface Chemistry and Catalysis, Ulm University, Albert-Einstein-Allee 47, D-89081, Ulm, Germany

<sup>c</sup> Karlsruhe Institute of Technology, Institute of Physical Chemistry, Fritz-Haber-Weg 2, D-76131, Karlsruhe, Germany

## ARTICLE INFO

### Article history:

Received 26 August 2019

Received in revised form

8 November 2019

Accepted 9 November 2019

Available online 10 November 2019

## ABSTRACT

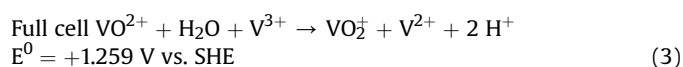
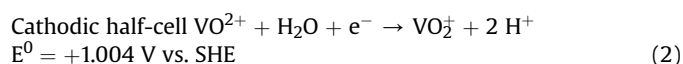
The identification and quantification of the side reactions in all-vanadium redox flow batteries are crucial to maintain its performance and to develop optimized materials. We altered the chemical composition and structure of the carbon felt electrodes by thermal treatment, chemical, and electrochemical aging, and also storing thermally treated felts for an extended period, which represent several stages in its life. The treated felts were evaluated regarding their affinity to side reactions and electrochemical activity towards both relevant vanadium redox couples ( $V^{2+}/V^{3+}$  and  $V^{4+}/V^{5+}$ ). Differential electrochemical mass spectrometry was utilized to track the potential dependant formation of  $CO_2$  and  $O_2$  on the positive electrode side and of  $H_2$  on the negative electrode side. Storing thermally treated felts for an extended period under ambient conditions results in a slightly decreased electrochemical performance and an increased  $CO_2$  formation due to oxidation by atmospheric oxygen. The  $V^{4+}/V^{5+}$  redox reaction is hampered on electrochemically aged carbon felts, while they show an increased electrochemical activity towards the  $V^{2+}/V^{3+}$  redox reaction, thus allowing recycling of aged cathode felts as an anode felt and therefore extending the overall lifetime of the carbon felt electrode.

© 2019 The Authors. Published by Elsevier Ltd. This is an open access article under the CC BY-NC-ND license (<http://creativecommons.org/licenses/by-nc-nd/4.0/>).

## 1. Introduction

Due to the gradual shift towards renewable energy sources, such as solar or wind power plants, the demand for stationary energy storage systems increases to compensate for the fluctuating power output of these energy sources. Redox flow batteries (RFBs) in general are a promising technology, since the power generation and energy storage capacities are decoupled, the manufacturing costs are potentially low, the design can be tailored to suit specific applications, and the response times to demand changes are comparatively fast [1–5]. As one specific type, vanadium redox flow batteries (VRFBs) utilize commonly two inexpensive carbon-based electrodes, an ion-exchange membrane and two vanadium-based electrolytes in the oxidation states (II)/(III) and (IV)/(V), which allows a high robustness towards electrolyte cross-contamination, relatively low environmental impact, and a long cycling life. The redox reactions occurring in the two half-cells are shown in equations (1) and (2),

and the full-cell equation (3), together with their corresponding redox potential [1,6]. Furthermore, several studies found the anodic half-cell to be the limiting reaction in a VRFB [7–10].

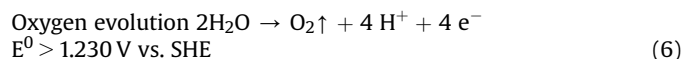
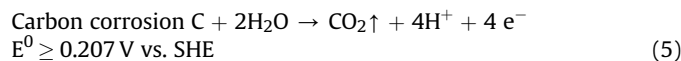
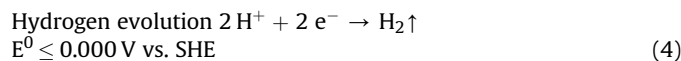


The most common electrode materials in VRFBs are carbon fiber-based materials, either as felts or as papers, due to their relatively low cost, decent electrical conductivity, and tunable activity. The latter two properties can be highly influenced by surface modifications such as varying the active surface area [11–15] or introducing functional groups by chemical [16–22] or thermal treatments [23–26]. Unfortunately, under the operating conditions of the VRFB, side reactions such as carbon corrosion and oxygen evolution at the cathode, and hydrogen evolution at the anode, lead

\* Corresponding author. Karlsruhe Institute of Technology, Helmholtz Institute Ulm, Helmholtzstraße 11, 89081, Ulm, Germany.

E-mail address: [roswitha.zeis@kit.edu](mailto:roswitha.zeis@kit.edu) (R. Zeis).

to significant performance losses [26]. The side reactions and their corresponding potentials with regard to the vanadium redox reactions are illustrated in Fig. 1(a), they can be described by the following reaction equations:



Due to their impact on the cell performance, the identification, quantification and systematic prevention of these side reactions gained considerable attention in the last decade. While earlier studies focussed on the positive electrode degradation and its dependence on the potential, temperature, or time and their detection [27,28], more recent ones discuss the side reactions on the negative electrode, assuming that this is the performance-limiting factor [29–33]. The impact of the pretreatment of different commercially available carbon felts on their surface composition, thermal stability and electrochemical behavior was addressed in detail in our preceding study [26]. In a subsequent study, we utilized differential electrochemical spectrometry (DEMS) to investigate the influence of the vanadium-containing electrolyte on the side reactions on carbon felt surfaces, and observed an increase of both,  $\text{CO}_2$  and  $\text{H}_2$  formation, in the presence of vanadium ions [34]. Furthermore, we did not find any indication of oxygen evolution (Eq. (6)) in the given potential window. This is in a good agreement with the findings of Liu et al., who studied the electrochemical corrosion of a graphite disc working electrode in sulfuric acid and vanadium-containing electrolyte [35]. They detected  $\text{O}_2$  formation only at potentials greater than 1.8 V vs. SHE.

To gain further insight on the side reactions occurring during the lifetime of carbon electrodes in VRFBs, we studied the influence of altering the chemical composition and structure of the carbon felt electrode surface by thermal treatment, chemical, and electrochemical aging, and evaluate the effect of storing the felt for an extended period under ambient conditions, as schematically summarized in Fig. 1(b). For that, we again utilize cyclic voltammetry and DEMS to detect the potential dependant formation rate of gases, which were formed due to side reactions, and combine these results with our previous findings focussing on the detailed characterization of resulting carbon materials [26] and a proof-of-concept DEMS study for the thermally activated carbon felt [34]. By applying a continuous flow of electrolyte via a model carbon felt electrode, a high utilization of the electrode surface area can be achieved, while continuously delivering reactant to the electrode surface and effectively removing the reaction products, which results in a well-defined mass transport limited current. The transport properties of carbon felt electrodes were addressed using a pore network modeling approach and X-ray computed tomography imaging in our previous publications [36–38] and in a preceding study [39]. These studies demonstrated the importance of the hydrophilicity of the functionalized carbon fibers for the permeability, diffusivity and invasion percolation of the porous medium. In contrast, under stopped-flow conditions, the electrolyte remains in the confined space within the model carbon felt electrode, allowing to perform regular cyclic voltammetry experiments and analyze the  $\text{V}^{4+}/\text{V}^{5+}$  and  $\text{V}^{2+}/\text{V}^{3+}$  redox couples quantitatively. In the following, after a description of the experimental procedures, we will discuss the electrochemical activity and reversibility of the vanadium redox reactions and stability of the carbon material in dependence upon

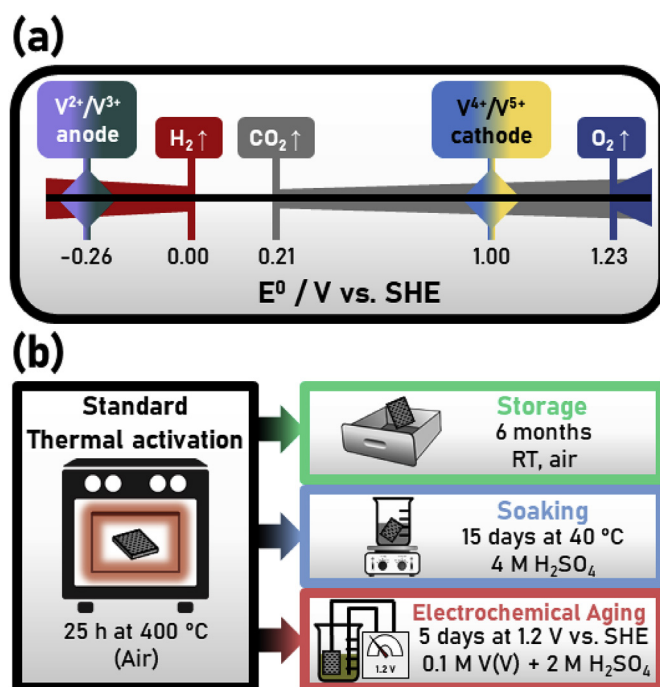


**Fig. 1.** (a) Possible reactions on carbon electrodes in VRFBs with their corresponding potentials. (b) Treatment procedures of the carbon felt in this study: A thermal activation at 400 °C for 25 h, followed by either 6 months of storage in a lab cabinet at room temperature and on-air, or soaking in 4 M  $\text{H}_2\text{SO}_4$  at 40 °C for 15 days, or electrochemical aging in 0.1 M  $\text{V}(\text{V}) + 2 \text{ M } \text{H}_2\text{SO}_4$  at 1.2 V vs. SHE for 5 days. (A colour version of this figure can be viewed online.)

the different treatment methods, which represent several stages during the lifetime of a carbon felt electrode in a VRFB.

## 2. Materials and methods

### 2.1. Preparation of materials

For these studies, we used the Rayon based graphitized carbon felt SIGRACELL® GFA6EA by SGL Carbon (Meitingen, Germany). Untreated, pristine felts are represented by a grey color in graphs throughout this study. To modify their physical and chemical properties, the pristine felts underwent several treatment procedures, as schematically shown in Fig. 1(b). The felts were first thermally treated at 400 °C for 25 h in an air atmosphere to introduce active sites as described previously in the literature [23,24,26,34], these materials are represented by a black color in the following graphs. After this, the felts underwent one of the following procedures, which represent several stages during the lifetime of carbon felt electrode in a VRFB:

- Storage in a lab cabinet for 6 months to evaluate the persistence of the thermal activation. The resulting materials are represented by green color in the following graphs.
- Soaking in 4 M  $\text{H}_2\text{SO}_4$  (technical, VWR) at 40 °C for 15 days to provide an insight into chemical aging during a typical single cell cycling experiment, uncoupled from the influence of vanadium ions and applied potential [26,40–42]. We based the higher concentration on current vanadium redox flow battery systems, which utilize total sulfate concentrations between 4 and 5 M [43]. The resulting materials are represented by a light blue color in graphs throughout this study.
- Electrochemical aging in 0.1 M  $\text{V}^{5+} + 2 \text{ M } \text{H}_2\text{SO}_4$  at 1.2 V vs. SHE for 5 days at room temperature, which induces high oxidative

stress in the carbon felts and is equivalent to the conditions at the positive electrode side of a fully charged VRFB [26,40,41,44]. The electrolyte was prepared by charging an appropriate vanadium (IV) electrolyte in a redox flow test cell (Scribner 857 test stand, Scribner Associates, North Carolina, USA), until a charging current of 2 mA/cm<sup>2</sup> was reached, where the battery is considered to be fully charged [26,40,45]. The resulting electrode materials are represented by red color in subsequent graphs.

We used a vanadium (IV) electrolyte in all electrochemical experiments, which was freshly prepared by dissolving an appropriate quantity of 5 mM VOSO<sub>4</sub> (VOSO<sub>4</sub>·5H<sub>2</sub>O, chemically pure, GfE) in 2 M H<sub>2</sub>SO<sub>4</sub> (Suprapur, Merck, diluted with purified Milli-Q water (18.2 MΩ cm)) [34]. Prior to each measurement, all felts were placed in purified water and sonicated for 5 min to remove contaminants.

## 2.2. Differential electrochemical spectrometry (DEMS) setup

A differentially pumped vacuum chamber with a quadrupole mass spectrometer (Pfeiffer Vacuum, QM 422) was utilized to monitor selected ion currents. The setup is described in more detail in Ref. [46]. A previously introduced, modified version of the dual thin-layer flow-through DEMS cell [34,47] was used to obtain potentiodynamic data and allow online detection of volatile species via a porous membrane (Scimat, 60 μm thick, 50% porosity and 0.2 μm pore diameter). The electrical contact of the felt was ensured by compressing the felt with a glassy carbon disc, which resulted in a relative compression of the felt by ~33%. The electrolyte flow was established by the hydrostatic pressure in the supply bottle at a constant flow rate of 6 μL/s. Two Pt wires at the inlet and outlet of the cell served as counter electrodes. A saturated calomel electrode connected to the outlet of the DEMS cell via a Teflon capillary was used as reference and all potentials were converted to SHE. Cyclic voltammetry measurements (scan rate 10 mV/s) were carried out using a potentiostat from Pine Instruments (AFRDE5), the data were acquired by the means of a home-written LabVIEW program.

Cyclic voltammograms were also recorded under stagnant electrolyte conditions, comparable to the situation in a standard half cell setup. In this case, however, we were not able to detect any volatile gasses produced during the reactions due to the configuration of the thin-layer cell used but allowing us the quantitative coulometric measurements of V<sup>4+</sup>/V<sup>5+</sup> or V<sup>2+</sup>/V<sup>3+</sup> redox couples at different potentials.

To investigate the impact of potential induced stress (carbon corrosion, hydrogen, and oxygen evolution), we utilized different potential regions. We used an oxidative potential range (–20 mV to +1580 mV), where we recorded CO<sub>2</sub> formation, as well as a broad potential range (–410 mV to +1580 mV), where we monitored of H<sub>2</sub>, O<sub>2</sub> and CO<sub>2</sub> formation. The mass spectrometric signals were background corrected to ensure comparability. To investigate the redox reaction of V<sup>2+</sup>/V<sup>3+</sup> in more detail, we selected a reductive potential range of –410 mV to 0 mV and stopped the electrolyte flow for that measurement. The material was cycled four to five times in the given potential window until a stable faradaic and mass current response was detected. In this work, only the final cyclic voltammograms and potential dependant mass current plots are shown.

## 3. Results and discussion

### 3.1. The influence of treatment methods on the CO<sub>2</sub> evolution in vanadium and base electrolyte

In Fig. 2 we show the potential dependant CO<sub>2</sub> formation under

electrolyte flow conditions (a) in 5 mM VOSO<sub>4</sub> in 2 M H<sub>2</sub>SO<sub>4</sub> and (b) in 2 M H<sub>2</sub>SO<sub>4</sub> base electrolyte, to assess the influence of the vanadium ions on differently treated carbon felts. Aiming at the analysis of the oxidation of V<sup>4+</sup> to V<sup>5+</sup> and the CO<sub>2</sub> evolution as the side reaction, the lower potential limit is set to 0 V to prevent H<sub>2</sub> evolution and a further reduction of the V<sup>4+</sup>. In the bottom part of Fig. 2(a), the typical steep increase in current is observed, which is related to the V<sup>4+</sup> oxidation. The onset potential is about 925 mV for thermally treated, cabinet stored and electrochemically aged carbon felts, whereas pristine and soaked felts show not only a much lower double layer capacity but also a higher onset potential of about 1055 mV, which correlates with a lower electrochemical activity. With increasing potential, a transport limited current between 2.1 and 3.8 mA was reached, which increased in the order: pristine < soaked < activated ≈ aged ≈ stored. The latter three electrodes show essentially similar currents, considering the different double layer capacities. The increase in the double layer capacities can be explained by the larger active surface area as a result of the increased wettability of the felts [37,48]. The increased electrochemical activity in the case of the treated samples leads to higher transport limited current.

The increase in current at potentials >1450 mV results from the oxidation of carbon to CO<sub>2</sub>, which is evidenced in the simultaneous mass spectrometric measurements (see top plot in Fig. 2(a)). As shown in previous studies, the thermal treatment reduces the CO<sub>2</sub> formation rate due to the removal of volatile components [26,40,49], whereas the storage time and electrochemical aging lead to a drastic increase, presumably due to partial oxidation of the surface by atmospheric oxygen or oxidative electrochemical stress, respectively. Furthermore, electrochemically aged felts show a redox peak of the quinone/hydroquinone couple at ca. 600 mV. A similar behavior is also observed for thermally treated and stored samples, but far less pronounced. The felts soaked in sulfuric acid show a slightly reduced CO<sub>2</sub> formation. This can be explained by an efficient oxidative removal of oxygen-containing surface groups in the warm sulfuric acid, which leaves only the most stable structures behind, as our previous work already indicated [26].

Comparison with the characteristics in 2 M H<sub>2</sub>SO<sub>4</sub> electrolyte illustrates the influence of the vanadium ions on the differently treated carbon felts. In Fig. 2(b) we show the cyclic voltammogram (bottom), as well as the potential dependent CO<sub>2</sub> ion current (top). Without any metallic redox couple in the electrolyte, the faradaic response solely results from surface groups, such as the quinone/hydroquinone redox couple. The currents gradually increase in the sequence pristine < soaked < thermally treated < stored < electrochemically aged, which is in agreement with previously reported data [26]. Compared to the vanadium-containing electrolyte, the quinone/hydroquinone redox couple is slightly more pronounced for electrochemically aged felts and slightly less for thermally treated and stored felts. With the potential approaching 1500 mV, the faradaic current increases exponentially, in full agreement with the CO<sub>2</sub> ion current shown in the upper part of Fig. 2(b). Both, CO<sub>2</sub> formation and faradaic current, increase in the order pristine < soaked < thermally treated < stored < electrochemically aged. This directly correlates with the increased double layer capacity and, thus, the increased surface area. Compared to CO<sub>2</sub> formation in the vanadium-containing electrolyte (Fig. 2(a)), we observe an almost doubled ion current for electrochemically aged felts in the absence of vanadium ions, whereas all other treatment procedures result in a reduced CO<sub>2</sub> formation. Furthermore, without vanadium ions, the electrochemically aged felts show a substantial CO<sub>2</sub> formation already at the onset potential of ca. 920 mV, which shifts to about 1050 mV in the presence of vanadium ions. Here, the V<sup>4+</sup> oxidation delivers the faradaic current at the given potential, while without vanadium ions present, the

highly oxidized surface [26] with a high surface area is further oxidized instead, resulting in a substantially higher overall  $\text{CO}_2$  formation. In contrast, on barely oxidized surfaces, such as pristine samples, we observe the previously reported [34] additional surface-oxidizing effect of vanadium ions. This effect is also observed on thermally treated and soaked carbon felts, albeit not as pronounced.

### 3.2. The influence of treatment methods on the vanadium redox reactions

To further investigate the influence of the treatment procedures on the vanadium redox reactions (Eq. (1) and (2)) we stopped the electrolyte flow and recorded cyclic voltammograms in 5 mM  $\text{VOSO}_4$  containing 2 M  $\text{H}_2\text{SO}_4$ , which are shown in Fig. 3. We evaluated the peak-to-peak separation ( $\Delta E$ ), the peak current ratio ( $I_A/I_C$ ) and the anodic to cathodic peak charge ratio ( $C_A/C_C$ ) for each redox couple and carbon felt sample and summarized the results in Table 1. These values give insight into the electrochemical reversibility and thus the overall performance of the material as an electrode in a VRFB [26,50,51].

As we have shown previously [26], thermal treatment enhances the electrochemical activity towards the  $\text{V}^{4+}/\text{V}^{5+}$  redox reaction. The decrease of  $\Delta E$  of the  $\text{V}^{4+}/\text{V}^{5+}$  redox couple from 362.2 mV for the pristine felt to 164.8 mV for the thermally treated felt indicates increased reversibility of the redox reaction. Both,  $I_A/I_C$ , as well as  $C_A/C_C$ , increase significantly to above 2 after thermal treatment and even reach almost 3 for stored felts. This results if more vanadium ions are oxidized than reduced at a given potential. The reason for that is the broad potential window of the cyclic voltammograms, where the lower potential limit is below the redox potential of the  $\text{V}^{2+}/\text{V}^{3+}$  reaction (standard potential for  $\text{V}^{2+}$  with an activity of 1,  $E^0 = -255$  mV, see Eq. (1) and Fig. 1(a)) and the sluggish redox reaction kinetics of the  $\text{V}^{3+}/\text{V}^{4+}$  couple ( $E^0 = 337$  mV), where the  $\text{V}^{3+}$  ions can only be oxidized at much higher potentials, which already overlap with the redox potential of the  $\text{V}^{4+}/\text{V}^{5+}$  reaction ( $E^0 = 1000$  mV, cf. Fig. 1(a)). This results in an instant oxidation of  $\text{V}^{3+}$  to  $\text{V}^{5+}$  with two electron transferred, which doubles both,  $I_A/I_C$  and  $C_A/C_C$ . This effect is visible in all felt electrodes, although the pristine and soaked felts show more evenly balanced current and charge ratios since only a small part of  $\text{V}^{4+}$  is reduced to  $\text{V}^{3+}$  or  $\text{V}^{2+}$ . This is reflected in the hardly noticeable  $\text{V}^{2+}/\text{V}^{3+}$  redox peak couple

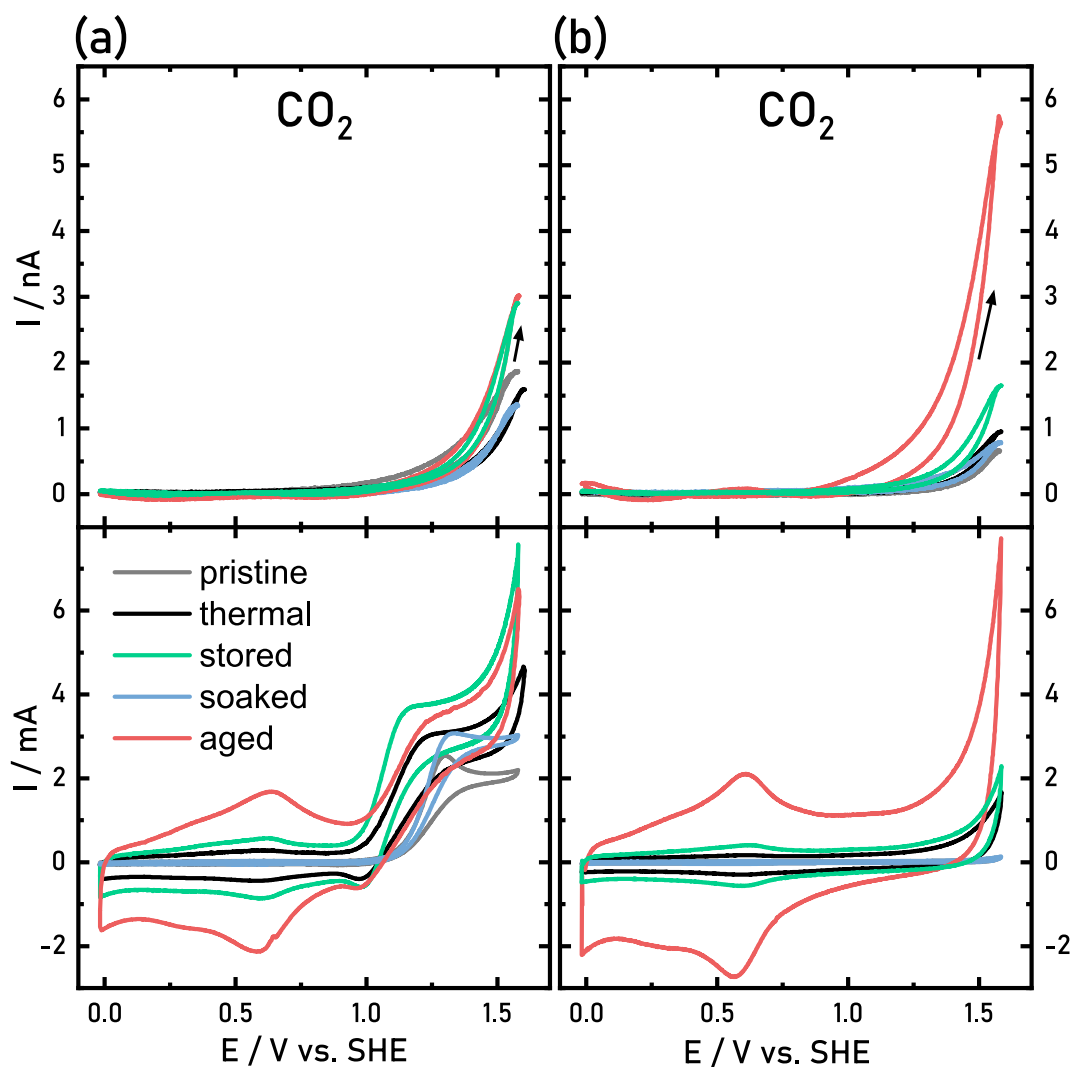


**Fig. 2.** CVs recorded on pristine (grey), thermally treated (black), cabinet stored (green), soaked in sulfuric acid (blue) and electrochemically aged (red) carbon felts under continuous flow conditions, showing the faradaic current response and the corresponding  $\text{CO}_2$  ion current in (a) a 5 mM  $\text{VOSO}_4$  in 2 M  $\text{H}_2\text{SO}_4$  electrolyte and in (b) a 2 M  $\text{H}_2\text{SO}_4$  base electrolyte. During all measurements, the potential scan rate was 10 mV/s and the flow rate of the respective electrolyte was about  $6 \mu\text{L/s}$ . (A colour version of this figure can be viewed online.)

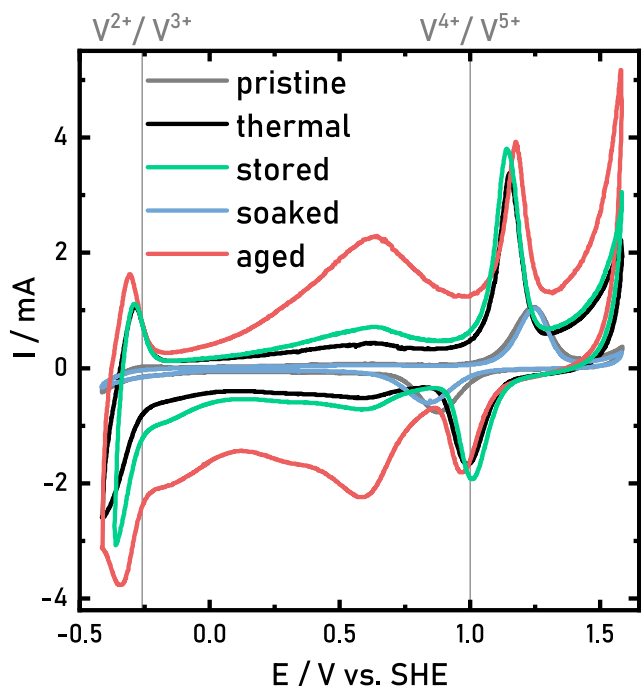


**Fig. 3.** CVs recorded on pristine (grey), thermally treated (black), cabinet stored (green), soaked in sulfuric acid (blue) and electrochemically aged (red) carbon felts under stopped flow conditions in 5 mM  $\text{VOSO}_4$  in 2 M  $\text{H}_2\text{SO}_4$  electrolyte with a potential scan rate of 10 mV/s. (A colour version of this figure can be viewed online.)

at very low potentials. Besides the enhanced vanadium redox activity, the thermal treatment also increases the double layer capacity via an increased surface area. Furthermore, it also shows a more pronounced quinone/hydroquinone redox couple at ca. 500 mV, which points to an increase of oxygen-containing functional groups on the carbon felt surface, in good agreement with our previous findings [26,34]. The effect of storing the felt in a lab cabinet for 6 months on the thermally induced electrochemical improvements in Fig. 3 is relatively low for the  $\text{V}^{4+}/\text{V}^{5+}$  redox reaction, showing only a slight increase in the double layer capacity and a more pronounced quinone/hydroquinone redox couple. The  $\text{V}^{2+}/\text{V}^{3+}$  redox reaction, on the other hand, shows a slightly reduced  $\Delta E$ . Minding that the felts were stored in an unsealed plastic bag in a closed lab cabinet, the two most probable interactions are oxidation by atmospheric oxygen and outgassing of  $\text{CO}_2$ , which was formed by oxidation of unstable surface groups.

Finally, soaking in sulfuric acid for 15 days or electrochemical aging in  $\text{V}^{5+}$  electrolyte for 5 days at 1.2 V vs. SHE heavily impacts the electrochemical behavior of the carbon felts. First of all, it is obvious that soaking a thermally treated sample reduces the reversibility of the  $\text{V}^{4+}/\text{V}^{5+}$  redox reaction, which is reflected in the increasing peak separation  $\Delta E$ , which increases from 164.8 for the freshly thermally treated sample to 402.8 mV, as shown in Table 1. Our present findings are in good agreement with the previous observation of a significant decrease in double-layer capacity, which mostly correlates with the surface area, while the charge ratio  $C_A/C_C$  approaches unity. In contrast, the electrochemical aging highly increases both, the quinone/hydroquinone redox peaks, as well as the double layer capacity, while it shows similar  $\Delta E$  and  $C_A/C_C$  values as the freshly thermally treated felt. Furthermore, the electrochemically aged and stored felts show a very low  $\Delta E$  for the  $\text{V}^{2+}/\text{V}^{3+}$  redox couple compared to thermally treated samples. The soaked sample did not show the distinct redox couple at low potentials, therefore we could not calculate the related

**Table 1**

Calculated data of the  $\text{V}^{4+}/\text{V}^{5+}$  and  $\text{V}^{2+}/\text{V}^{3+}$  redox peaks for the different carbon samples, retrieved from the cyclic voltammetry in the full (ca.  $-0.4 - 1.6$  V) potential range without electrolyte flow.

Felt type	Redox couple	$\Delta E$ [mV]	$I_A/I_C$	$C_A/C_C$
Pristine	$\text{V}^{4+}/\text{V}^{5+}$	362.2	1.41	1.34
Thermal	$\text{V}^{4+}/\text{V}^{5+}$	164.8	2.31	2.54
Stored	$\text{V}^{4+}/\text{V}^{5+}$	122.4	2.11	2.95
Soaked	$\text{V}^{4+}/\text{V}^{5+}$	402.8	1.71	1.28
Aged	$\text{V}^{4+}/\text{V}^{5+}$	213.9	3.77	1.97
Pristine	$\text{V}^{2+}/\text{V}^{3+}$	181.3	0.04	0.08
Thermal	$\text{V}^{2+}/\text{V}^{3+}$	127.6	0.35	0.19
Stored	$\text{V}^{2+}/\text{V}^{3+}$	77.2	0.27	0.09
Soaked	$\text{V}^{2+}/\text{V}^{3+}$	-	-	-
Aged	$\text{V}^{2+}/\text{V}^{3+}$	38.2	0.44	0.28

electrochemical data for this sample. On the other hand, both pristine and soaked carbon felt electrodes exhibit the largest  $\Delta E$ , which could also be related to a measured Ohmic loss due to an increased hydrophobicity caused by the developed functional groups [26].

### 3.3. The influence of treatment methods on the $\text{H}_2$ , $\text{O}_2$ and $\text{CO}_2$ evolution

We again enabled when the electrolyte flow to simultaneously track the potential dependent gas evolution of  $\text{CO}_2$ , and now additionally,  $\text{H}_2$ , and  $\text{O}_2$ . The cyclic voltammograms and the corresponding ion currents, recorded in (a) 5 mM  $\text{VOSO}_4$  in 2 M  $\text{H}_2\text{SO}_4$  and in (b) 2 M  $\text{H}_2\text{SO}_4$  base electrolyte, are shown in Fig. 4. The  $\text{CO}_2$  formation of the pristine felt is much lower compared to the same felt with higher potential limit (cf. Fig. 2(a)), which points towards an increased surface stability against oxidation after thorough reduction. Looking at the thermally treated and stored carbon felts, they show nearly identical transport limited currents of around 3 mA, and also similar  $\text{H}_2$  formation rates of about 0.2 nA, and both values are higher in comparison with the pristine carbon felt. Both, soaking in sulfuric acid and electrochemical aging, show a lower transport limited current (both ca. 2 mA). The  $\text{CO}_2$  formation rate of the stored felt is unaffected by the change of the lower potential limit and is still higher than that of the freshly thermally treated sample. A similar trend is also visible for the  $\text{CO}_2$  mass spectrometric signals: a lower potential limit – and therefore a more reduced carbon surface – does not affect the maximum  $\text{CO}_2$  formation at 1.5 V for thermally treated felts, whereas soaked and electrochemically aged felts show a reduced  $\text{CO}_2$  ion current of about 80% at 1.5 V, as would be expected for materials, which underwent a highly oxidizing treatment. It is worth mentioning that for the thermally treated and electrochemically aged felts, we already observe an increased  $\text{CO}_2$  ion current at 0.5 V, which corresponds to the oxidation of hydroquinone groups on the carbon surface. For the oxygen evolution, we observe no significant changes, independent of the treatment procedure, since the upper potential limit is not high enough to generate measurable amounts of oxygen. This corresponds well with findings of previous studies [34,35].

$\text{H}_2$  evolution is most pronounced for thermally treated and stored felts (cf. Fig. 4(a)), while both soaked and electrochemically aged felts show about 50% less  $\text{H}_2^+$  ion current. Interestingly, the electrochemically aged felts show about the same faradaic current at  $-0.45$  V as the thermally treated samples, while evolving less  $\text{H}_2$ . This again points towards an increased electrochemical activity of the  $\text{V}^{2+}/\text{V}^{3+}$  redox reaction, since more electrons are utilized for the vanadium (III) reduction rather than for  $\text{H}_2$  evolution. To verify this

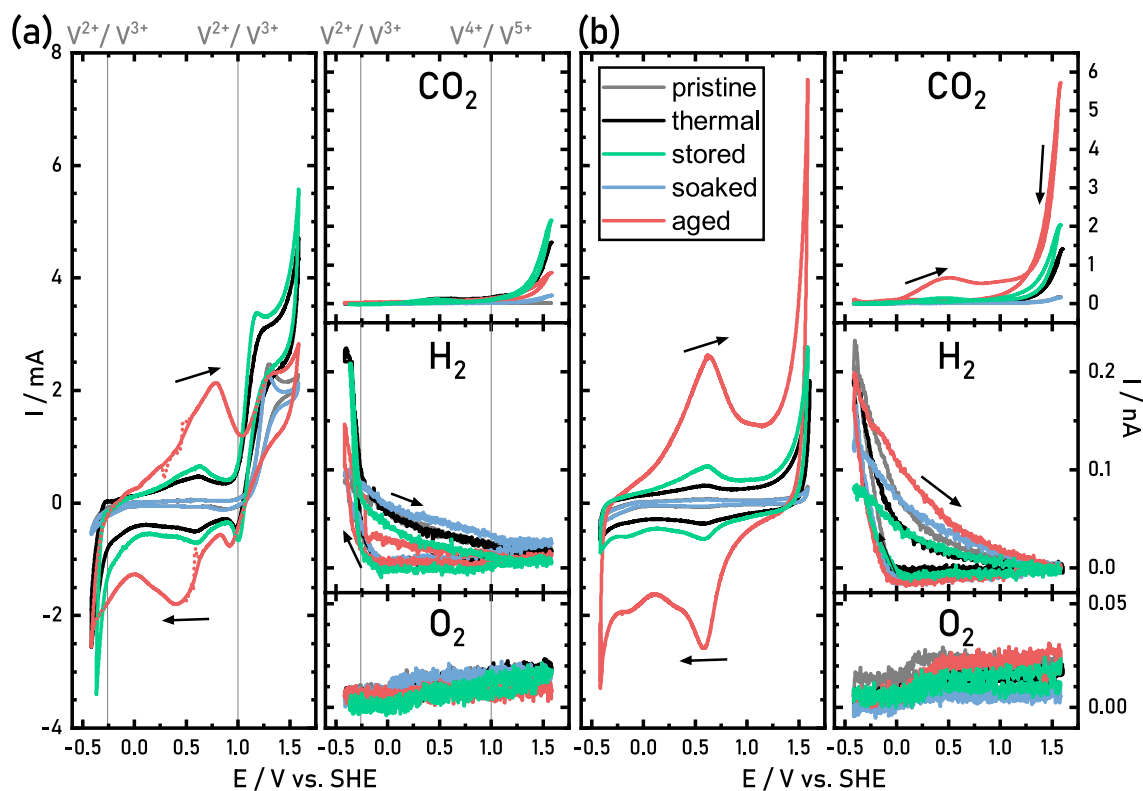


**Fig. 4.** CVs and the corresponding ion current plots of  $\text{CO}_2$ ,  $\text{H}_2$  and  $\text{O}_2$  recorded on pristine (grey), thermally treated (black), cabinet stored (green), soaked in sulfuric acid (blue) and electrochemically aged (red; dotted: raw data; solid: fit) carbon felts under continuous flow conditions, showing the  $\text{V}^{4+}$  oxidation,  $\text{V}^{3+}$  reduction, and the corresponding gas evolution currents in (a) a 5 mM  $\text{VOSO}_4$  in 2 M  $\text{H}_2\text{SO}_4$  electrolyte and in (b) a 2 M  $\text{H}_2\text{SO}_4$  base electrolyte. The grey vertical lines in (a) mark the redox potential of the  $\text{V}^{2+}/\text{V}^{3+}$  ( $-0.26$  V) and  $\text{V}^{4+}/\text{V}^{5+}$  (1.00 V) redox couple, respectively. During all measurements, the potential scan rate was 10 mV/s and the flow rate of the electrolyte was about 6  $\mu\text{L}/\text{s}$ . The scales of the cyclic voltammograms and potential dependant mass currents are identical in (a) and (b). (A colour version of this figure can be viewed online.)

observation in more detail, we set the potential window between  $-0.45$  V and 0 V vs. SHE and stopped the electrolyte flow. The stable cyclic voltammograms obtained after 3 cycles are shown in Fig. 5. The double-layer capacities follow the same trends, when the carbon surface is largely reduced, compared to the previous scans to higher potentials (Fig. 3). In Fig. 5, thermally treated felts already show a decent reversibility, resulting in a  $\Delta E$  of 62.6 mV, but a  $C_A/C_C$  ratio of below one, which confirms the relatively high amount of  $\text{H}_2$  formation. Soaking in sulfuric acid also diminishes the electrochemical activity of the  $\text{V}^{2+}/\text{V}^{3+}$  redox reaction on the carbon felt ( $\Delta E = 237.1$  mV,  $I_A/I_C = 0.49$ ,  $C_A/C_C = 1.01$ ). The electrochemical aging shows a peak-to-peak separation of 27.5 mV, which is at the first glance surprisingly well below the theoretical value of 59 mV per transferred electron, but can be explained by the electrode porosity, which influences  $\Delta E$  [37,48,52,53]. Moving on to the electrochemical aging treatment, the peak current ratio does not change significantly, only the absolute peak currents are slightly higher due to the increased surface area. Although the felts are corroded by the electrochemical aging, which represents aging at the positive electrode, and lose the electrochemical activity towards the  $\text{V}^{4+}/\text{V}^{5+}$  redox reaction, they show a slightly improved activity towards the  $\text{V}^{2+}/\text{V}^{3+}$  redox reaction. This we relate again to the higher double-layer capacity and thus to the larger surface area. As a practical consequence, by re-using degraded felts of the positive half cell in the negative half cell, it could be possible to extend the overall lifetime of the VRFB electrodes, although further work (e.g. full-cell tests) is necessary, to study this effect in detail.

In sulfuric acid as flowing base electrolyte, the  $\text{CO}_2$  ion current follows the same trend as for the smaller potential window in Fig. 2(b) and in the faradaic current responses. We observe an

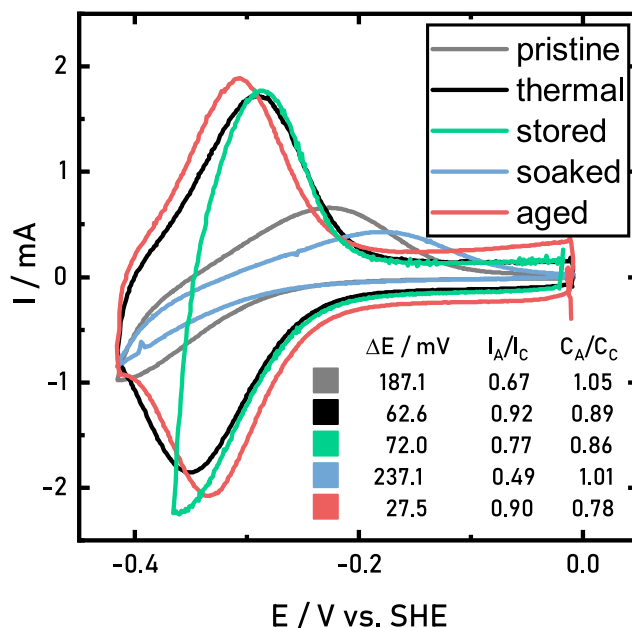


**Fig. 5.** CVs recorded on pristine (grey), thermally treated (black), cabinet stored (green), soaked in sulfuric acid (blue) and electrochemically aged (red) carbon felts under stopped flow conditions, showing the  $\text{V}^{2+}/\text{V}^{3+}$  redox couple in 5 mM  $\text{VOSO}_4$  in 2 M  $\text{H}_2\text{SO}_4$  electrolyte (potential scan rate 10 mV/s). The inserted table shows the calculated peak currents of the  $\text{V}^{2+}/\text{V}^{3+}$  redox peak for the different carbon samples. (A colour version of this figure can be viewed online.)

increased CO<sub>2</sub> formation during the hydroquinone oxidation for all samples, which starts already at around 0 V. This is especially noticeable for electrochemically aged felts and, less pronounced, for the cabinet stored samples. Looking at the H<sub>2</sub><sup>+</sup> ion current, the pristine samples show the highest value, followed by the thermally treated, electrochemically aged and soaked felts. Cabinet stored samples, on the other hand, show a lower H<sub>2</sub> evolution in sulfuric acid, indicating a high influence of the vanadium ions on the activity of carbon felt surfaces for H<sub>2</sub> evolution. The XPS analysis in our previous report [26] showed that the <sup>O=C/O-C</sup> ratio of pristine samples are close to 1 with an O/C ratio of 0.34, whereas the treated samples have <sup>O=C/O-C</sup> ratios of around 0.5 with O/C ratios of 0.26 (thermally treated), 0.47 (soaked), and 0.41 (electrochemically aged). Furthermore, electrochemically aged felts show a very high <sup>sp<sup>2</sup>/sp<sup>3</sup></sup> ratio of 12 and Raman measurements provide a I<sub>D</sub>/I<sub>G</sub> ratio of 1.43, which indicates the highest graphitic content in comparison with the other samples. Combining this with our present findings, we suggest that a high content of single-bonded O enhances the activity of the carbon felt for H<sub>2</sub> evolution, and also that for the oxidation of V<sup>4+</sup> ions, whereas a high content of double-bonded O and graphitic carbon increases the activity towards the V<sup>2+</sup>/V<sup>3+</sup> redox reaction. The O<sub>2</sub> evolution shows a slight, step-like decrease between 0 and 0.5 V, which can be explained by the reduction of residing amounts in the flowing electrolyte.

#### 4. Conclusions

Investigating the influence of different treatment procedures of commercially available carbon felt electrodes for VRFBs on their electrochemical activity and their susceptibility towards side reactions such as carbon corrosion and hydrogen evolution by electrochemical and online mass spectrometric measurements, we could show that thermally treated felts expectedly exhibit an increased electrochemical activity, but also a higher affinity to side reactions compared to pristine felts. This kind of activation process is anyway necessary to achieve usable performance in VRFBs, although this material by itself is very prone to side reactions and is therefore not fully utilized. Storing these thermally treated felts in a lab cabinet for an extended period led to increased carbon corrosion due to oxidation by atmospheric oxygen. Although freshly thermally activated carbon felts show a slightly better performance, the difference to stored felts after activation is marginal, which implies that stored felts can still be used, without resulting in significant lower performance. The influence of the oxidizing sulfuric acid was shown by soaking the thermally treated felts in it, which results in reduced electrochemical activity, but also reduced side reactions. The chemical oxidation without the influence of vanadium ions and applied potential is already relatively high, which shows that the felts could possibly be modified to withstand the harsh environment. By electrochemically aging carbon felts, the electrochemical activity towards the redox reaction in the catholyte decreases, as well as its affinity to side reactions. However, these electrochemically aged felts exhibit an increased electrochemical performance in the anolyte, which points towards a possible recycling path for aged cathodic carbon felts and therefore extends the lifetime of the electrodes in a VRFB.

#### Declaration of competing interest

The authors declare that they have no known competing financial interests or personal relationships that could have appeared to influence the work reported in this paper.

#### Acknowledgments

We gratefully acknowledge financial support by the German Federal Ministry of Education and Research (BMBF) in the project 03X4636C and the Impuls-und Vernetzungsfonds der Helmholtz Gesellschaft (Young Investigator Group project VH-NG-616). We gratefully acknowledge SGL Carbon for the supply of SIGRACELL® carbon felts. This work contributes to the research performed at CELEST (Center for Electrochemical Energy Storage Ulm-Karlsruhe).

#### References

- [1] G.L. Soloveichik, Flow batteries: current status and trends, *Chem. Rev.* 115 (2015) 11533–11558, <https://doi.org/10.1021/cr500720t>.
- [2] L. Li, X. Wei, B. Li, Z. Yang, Q. Luo, W. Wang, Recent progress in redox flow battery research and development, *Adv. Funct. Mater.* 23 (2012) 970–986, <https://doi.org/10.1002/adfm.201200694>.
- [3] M.H. Chakrabarti, F.S. Mjalli, M. Skyllas-Kazacos, M. Saleem, S.A. Hajimolana, Progress in flow battery research and development, *J. Electrochem. Soc.* 158 (2011) R55, <https://doi.org/10.1149/1.3599565>.
- [4] A.Z. Weber, M.M. Mench, J.P. Meyers, P.N. Ross, J.T. Gostick, Q. Liu, Redox flow batteries: a review, *J. Appl. Electrochem.* 41 (2011) 1137–1164, <https://doi.org/10.1007/s10800-011-0348-2>.
- [5] C. Minke, T. Turek, Materials, system designs and modelling approaches in techno-economic assessment of all-vanadium redox flow batteries – a review, *J. Power Sources* 376 (2018) 66–81, <https://doi.org/10.1016/j.jpowsour.2017.11.058>.
- [6] T. Liu, X. Li, H. Zhang, J. Chen, Progress on the electrode materials towards vanadium flow batteries (VFBs) with improved power density, *J. Energy Chem.* 27 (2018) 1292–1303, <https://doi.org/10.1016/j.jechem.2018.07.003>.
- [7] Y. Wu, R. Holze, Electrocatalysis at electrodes for VanadiumRedox flow batteries, *Batteries* 4 (2018) 47, <https://doi.org/10.3390/batteries4030047>.
- [8] W. Wang, X. Fan, Y. Qin, J. Liu, C. Yan, C. Zeng, The reduction reaction kinetics of vanadium(V) in acidic solutions on a platinum electrode with unusual difference compared to carbon electrodes, *Electrochim. Acta* 283 (2018) 1313–1322, <https://doi.org/10.1016/j.electacta.2018.07.071>.
- [9] M.A. Goulet, M. Eikerling, E. Kjeang, Direct measurement of electrochemical reaction kinetics in flow-through porous electrodes, *Electrochem. Commun.* 57 (2015) 14–17, <https://doi.org/10.1016/j.elecom.2015.04.019>.
- [10] J. Friedl, U. Stimming, Determining electron transfer kinetics at porous electrodes, *Electrochim. Acta* 227 (2017) 235–245, <https://doi.org/10.1016/j.electacta.2017.01.010>.
- [11] I. Mustafa, A. Al Shehhi, A. Al Hammadi, R. Susantyoko, G. Palmisano, S. Almheiri, Effects of carbonaceous impurities on the electrochemical activity of multiwalled carbon nanotube electrodes for vanadium redox flow batteries, *Carbon* N. Y. 131 (2018) 47–59, <https://doi.org/10.1016/j.carbon.2018.01.069>.
- [12] I. Taurino, S. Carrara, M. Giorcelli, A. Tagliaferro, G. De Micheli, Comparison of two different carbon nanotube-based surfaces with respect to potassium ferricyanide electrochemistry, *Surf. Sci.* 606 (2012) 156–160, <https://doi.org/10.1016/j.susc.2011.09.001>.
- [13] P. Han, Y. Yue, Z. Liu, W. Xu, L. Zhang, H. Xu, S. Dong, G. Cui, Graphene oxide nanosheets/multi-walled carbon nanotubes hybrid as an excellent electrocatalytic material towards VO<sub>2</sub><sup>+</sup>/VO<sub>2</sub><sup>+</sup> redox couples for vanadium redox flow batteries, *Energy Environ. Sci.* 4 (2011) 4710, <https://doi.org/10.1039/c1ee01776d>.
- [14] L. Wei, T.S. Zhao, G. Zhao, L. An, L. Zeng, A high-performance carbon nanoparticle-decorated graphite felt electrode for vanadium redox flow batteries, *Appl. Energy* 176 (2016) 74–79, <https://doi.org/10.1016/j.apenergy.2016.05.048>.
- [15] J. Friedl, C.M. Bauer, A. Rinaldi, U. Stimming, Electron transfer kinetics of the VO<sub>2</sub><sup>+</sup>/VO<sub>2</sub><sup>+</sup> - Reaction on multi-walled carbon nanotubes, *Carbon* N. Y. 63 (2013) 228–239, <https://doi.org/10.1016/j.carbon.2013.06.076>.
- [16] H.J. Lee, D. Kil, H. Kim, Synthesis of activated graphite felt using consecutive post-treatments for vanadium redox flow batteries, *J. Electrochem. Soc.* 163 (2016) A2586–A2591, <https://doi.org/10.1149/2.0531613jes>.
- [17] Z. He, L. Shi, J. Shen, Z. He, S. Liu, Effects of nitrogen doping on the electrochemical performance of graphite felts for vanadium redox flow batteries, *Int. J. Energy Res.* 39 (2015) 709–716, <https://doi.org/10.1002/er.3291>.
- [18] H. Zhang-Xing, L. Jian-Lei, H. Zhen, L. Su-Qin, Nitrogen-doped carbon paper as electrodes for vanadium redox flow batteries, *J. Inorg. Mater.* 30 (2015) 779, <https://doi.org/10.15541/jim20140656>.
- [19] Z. He, Y. Jiang, Y. Li, L. Wang, L. Dai, Boosting the electrocatalytic performance of carbon nanotubes toward V(V)/V(IV) reaction by sulfonation treatment, *Int. J. Energy Res.* 42 (2018) 1625–1634, <https://doi.org/10.1002/er.3958>.
- [20] Z. He, Y. Jiang, Y. Wei, C. Zhao, F. Jiang, L. Li, H. Zhou, W. Meng, L. Wang, L. Dai, N,P co-doped carbon microsphere as superior electrocatalyst for VO<sub>2</sub><sup>+</sup>/VO<sub>2</sub><sup>+</sup> redox reaction, *Electrochim. Acta* 259 (2018) 122–130, <https://doi.org/10.1016/j.electacta.2017.10.169>.
- [21] A.M. Schwenke, T. Janoschka, C. Stolze, N. Martin, S. Hoepfner, U.S. Schubert, Microwave-assisted preparation of carbon nanofiber-functionalized graphite felts as electrodes for polymer-based redox-flow batteries, *J. Power Sources*

- 335 (2016) 155–161, <https://doi.org/10.1016/j.jpowsour.2016.09.121>.
- [22] D. Dixon, D.J. Babu, J. Langner, M. Bruns, L. Pfaffmann, A. Bhaskar, J.J. Schneider, F. Scheiba, H. Ehrenberg, Effect of oxygen plasma treatment on the electrochemical performance of the rayon and polyacrylonitrile based carbon felt for the vanadium redox flow battery application, *J. Power Sources* 332 (2016) 240–248, <https://doi.org/10.1016/j.jpowsour.2016.09.070>.
- [23] B. Sun, M. Skyllas-Kazacos, Modification of graphite electrode materials for vanadium redox flow battery application—I. Thermal treatment, *Electrochim. Acta* 37 (1992) 1253–1260, [https://doi.org/10.1016/0013-4686\(92\)85064-R](https://doi.org/10.1016/0013-4686(92)85064-R).
- [24] A.M. Pezeshki, J.T. Clement, G.M. Veith, T.A. Zawodzinski, M.M. Mench, High performance electrodes in vanadium redox flow batteries through oxygen-enriched thermal activation, *J. Power Sources* 294 (2015) 333–338, <https://doi.org/10.1016/j.jpowsour.2015.05.118>.
- [25] J. Noack, J. Tübke, A comparison of materials and treatment of materials for vanadium redox flow battery, in: *ECS Trans*, 2010, pp. 235–245, <https://doi.org/10.1149/1.3414022>.
- [26] L. Eifert, R. Banerjee, Z. Jusys, R. Zeis, Characterization of carbon felt electrodes for vanadium redox flow batteries: impact of treatment methods, *J. Electrochem. Soc.* 165 (2018) A2577–A2586, <https://doi.org/10.1149/2.0531811jes>.
- [27] H. Liu, Q. Xu, C. Yan, Y. Qiao, Corrosion behavior of a positive graphite electrode in vanadium redox flow battery, *Electrochim. Acta* 56 (2011) 8783–8790, <https://doi.org/10.1016/j.electacta.2011.07.083>.
- [28] Z. Wu, H. Zhou, L. Liu, Z. Li, X. Qiu, J. Xi, H. Zhou, Z. Wu, X. Qiu, Rapid detection of the positive side reactions in vanadium flow batteries, *Appl. Energy* 185 (2016) 452–462, <https://doi.org/10.1016/j.apenergy.2016.10.141>.
- [29] A. Fetyan, G.A. El-Nagar, I. Lauerermann, M. Schnucklake, J. Schneider, C. Roth, Detrimental role of hydrogen evolution and its temperature-dependent impact on the performance of vanadium redox flow batteries, *J. Energy Chem.* (2018), <https://doi.org/10.1016/j.jechem.2018.06.010>.
- [30] P. Mazur, J. Mrlik, J. Pocedic, J. Vrana, J. Dundalek, J. Kosek, T. Bystron, Effect of graphite felt properties on the long-term durability of negative electrode in vanadium redox flow battery, *J. Power Sources* 414 (2019) 354–365, <https://doi.org/10.1016/j.jpowsour.2019.01.019>.
- [31] L. Wei, T.S.S. Zhao, Q. Xu, X.L.L. Zhou, Z.H.H. Zhang, In-situ investigation of hydrogen evolution behavior in vanadium redox flow batteries, *Appl. Energy* 190 (2017) 1112–1118, <https://doi.org/10.1016/j.apenergy.2017.01.039>.
- [32] S.M. Taylor, A. Pátru, D. Perego, E. Fabbri, T.J. Schmidt, Influence of carbon material properties on activity and stability of the negative electrode in vanadium redox flow batteries: a model electrode study, *ACS Appl. Energy Mater.* 1 (2018) 1166–1174, <https://doi.org/10.1021/acsaem.7b00273>.
- [33] E. Agar, C.R. Dennison, K.W. Knehr, E.C. Kumbur, Identification of performance limiting electrode using asymmetric cell configuration in vanadium redox flow batteries, *J. Power Sources* 225 (2013) 89–94, <https://doi.org/10.1016/j.jpowsour.2012.10.016>.
- [34] L. Eifert, Z. Jusys, R. Banerjee, R.J. Behm, R. Zeis, Differential electrochemical mass spectrometry of carbon felt electrodes for vanadium redox flow batteries, *ACS Appl. Energy Mater.* (2018), <https://doi.org/10.1021/acsaem.8b01550>.
- [35] H. Liu, Q. Xu, C. Yan, On-line mass spectrometry study of electrochemical corrosion of the graphite electrode for vanadium redox flow battery, *Electrochem. Commun.* 28 (2013) 58–62, <https://doi.org/10.1016/j.elecom.2012.12.011>.
- [36] R. Banerjee, N. Bevilacqua, L. Eifert, R. Zeis, Characterization of carbon felt electrodes for vanadium redox flow batteries – a pore network modeling approach, *J. Energy Storage* 21 (2019) 163–171, <https://doi.org/10.1016/j.est.2018.11.014>.
- [37] N. Bevilacqua, L. Eifert, R. Banerjee, K. Köble, T. Faragó, M. Zuber, A. Bazylak, R. Zeis, Visualization of electrolyte flow in vanadium redox flow batteries using synchrotron X-ray radiography and tomography – impact of electrolyte species and electrode compression, *J. Power Sources* 439 (2019), 227071, <https://doi.org/10.1016/j.jpowsour.2019.227071>.
- [38] R. Banerjee, N. Bevilacqua, A. Mohseninia, B. Wiedemann, F. Wilhelm, J. Scholta, R. Zeis, Carbon felt electrodes for redox flow battery: impact of compression on transport properties, *J. Energy Storage* 26 (2019), 100997, <https://doi.org/10.1016/j.est.2019.100997>.
- [39] F. Tariq, J. Rubio-García, V. Yufit, A. Bertei, B.K. Chakrabarti, A. Kucernak, N. Brandon, Uncovering the mechanisms of electrolyte permeation in porous electrodes for redox flow batteries through real time in-situ 3D imaging, *Sustain. Energy Fuels* 2 (2018) 2068–2080, <https://doi.org/10.1039/C8SE00174J>.
- [40] O. Nibel, S.M. Taylor, A. Pátru, E. Fabbri, L. Gubler, T.J. Schmidt, Performance of different carbon electrode materials: insights into stability and degradation under real vanadium redox flow battery operating conditions, *J. Electrochem. Soc.* 164 (2017) A1608–A1615, <https://doi.org/10.1149/2.1081707jes>.
- [41] I. Derr, M. Bruns, J. Langner, A. Fetyan, J. Melke, C. Roth, Degradation of all-vanadium redox flow batteries (VRFB) investigated by electrochemical impedance and X-ray photoelectron spectroscopy: Part 2 electrochemical degradation, *J. Power Sources* 325 (2016) 351–359, <https://doi.org/10.1016/j.jpowsour.2016.06.040>.
- [42] M.G. George, H. Liu, D. Muirhead, R. Banerjee, N. Ge, P. Shrestha, J. Lee, S. Chevalier, J. Hinebaugh, M. Messerschmidt, R. Zeis, J. Scholta, A. Bazylak, Accelerated degradation of polymer electrolyte membrane fuel cell gas diffusion layers, *J. Electrochem. Soc.* 164 (2017) F714–F721, <https://doi.org/10.1149/2.0091707jes>.
- [43] S. Roe, C. Menictas, M. Skyllas-Kazacos, A high energy density vanadium redox flow battery with 3 M vanadium electrolyte, *J. Electrochem. Soc.* 163 (2016) A5023–A5028, <https://doi.org/10.1149/2.0041601jes>.
- [44] J. Langner, J. Melke, H. Ehrenberg, C. Roth, Determination of overpotentials in all vanadium redox flow batteries, *ECS Trans.* 58 (2014) 1–7, <https://doi.org/10.1149/05837.0001ecst>.
- [45] D.S. Aaron, Q. Liu, Z. Tang, G.M. Grim, A.B. Papandrew, A. Turhan, T.A. Zawodzinski, M.M. Mench, Dramatic performance gains in vanadium redox flow batteries through modified cell architecture, *J. Power Sources* 206 (2012) 450–453, <https://doi.org/10.1016/j.jpowsour.2011.12.026>.
- [46] M. Heinen, Y.X. Chen, Z. Jusys, R.J. Behm, In situ ATR-FTIRS coupled with on-line DEMS under controlled mass transport conditions—A novel tool for electrocatalytic reaction studies, *Electrochim. Acta* 52 (2007) 5634–5643, <https://doi.org/10.1016/j.electacta.2007.01.055>.
- [47] Z. Jusys, H. Massong, H. Baltruschat, A new approach for simultaneous DEMS and EQCM: electro-oxidation of adsorbed CO on Pt and Pt-Ru, *J. Electrochem. Soc.* 146 (1999) 1093, <https://doi.org/10.1149/1.1391726>.
- [48] M.A. Goulet, M. Skyllas-Kazacos, E. Kjeang, The importance of wetting in carbon paper electrodes for vanadium redox reactions, *Carbon* N. Y. 101 (2016) 390–398, <https://doi.org/10.1016/j.carbon.2016.02.011>.
- [49] S. Zhong, C. Padeste, M. Kazacos, M. Skyllas-Kazacos, Comparison of the physical, chemical and electrochemical properties of rayon- and polyacrylonitrile-based graphite felt electrodes, *J. Power Sources* 45 (1993) 29–41, [https://doi.org/10.1016/0378-7753\(93\)80006-B](https://doi.org/10.1016/0378-7753(93)80006-B).
- [50] M. Park, J. Ryu, W. Wang, J. Cho, Material design and engineering of next-generation flow-battery technologies, *Nat. Rev. Mater.* 2 (2016), 16080, <https://doi.org/10.1038/natrevmats.2016.80>.
- [51] K. Kinoshita, *Carbon: Electrochemical and Physicochemical Properties*, Wiley, 1988.
- [52] C. Punctk, M.A. Pope, I.A. Aksay, On the electrochemical response of porous functionalized graphene electrodes, *J. Phys. Chem. C* 117 (2013) 16076–16086, <https://doi.org/10.1021/jp405142k>.
- [53] M. Schnucklake, A. Fetyan, G. El-Nagar, J. Schneider, C. Roth, P. Kubella, E. Bulczak, I. Derr, M. Gebhard, Degradation phenomena of bismuth-modified felt electrodes in VRFB studied by electrochemical impedance spectroscopy, *Batteries* 5 (2019) 16, <https://doi.org/10.3390/batteries5010016>.